

Gluon distributions and color charge correlations in a saturated light-cone wavefunction¹

A.H. Mueller

Physics Department, Columbia University
New York, N.Y. 10027 USA

Abstract

We describe the light-cone wavefunction in the saturation regime in terms of the density of gluons per unit of transverse phase space, the occupation number, and in terms of the color charge correlator. The simple McLerran-Venugopalan model gives what are claimed to be general results for the phase space gluon density, but it does not well describe the general case for the charge correlator. We derive the general momentum dependence and rapidity dependence of the color charge correlator which exhibits strong color shielding. A simple physical picture which leads to these general results is described.

1 Introduction

Our object in this paper is to describe what the light-cone wavefunction looks like in the saturation regime, that is when the occupation numbers of gluons are large. What we attempt to describe is the density of gluons and the color charge correlator as a function of rapidity and transverse momentum. We shall carry out this description first for the McLerran-Venugopalan model[1, 2, 3], then for an unsaturated BFKL[4, 5] light-cone wavefunction and finally for a more general saturated wavefunction, both for fixed coupling and for running coupling.

¹This research is supported in part by the US Department of Energy.

For the gluon density in phase space we find the result that $\frac{dxG}{d^2bd^2\ell_\perp}$ is proportional to $\frac{N_c^2-1}{\alpha N_c} \ell n[Q_s^2(Y)/\ell_\perp^2]$ in all the saturation models. We believe this to be a very general result which follows straightforwardly from the physical picture we give in Sec.6.

The color charge correlator $\rho(\ell_\perp, Y)$, defined below in (17), is a constant in the McLerran-Venugopalan model reflecting the fact that the elementary charges are completely uncorrelated in that model on scales small compared to one fermi. We note that the first gluonic corrections to the model, calculated in Sec.2 begin to show charge shielding. Charge shielding is clearly visible in the BFKL wavefunction and in saturated wavefunctions produced from BFKL evolution. In the latter case, both for fixed coupling and for running coupling, $\frac{d}{dY}\rho(\ell_\perp, Y) = \frac{N_c^2-1}{\pi}\ell_\perp^2$ in the saturation region, and the proportionality to ℓ_\perp^2 means that charge shielding is as complete as it can be. That is when measured on a scale $\Delta x_\perp \sim 1/\ell_\perp$ all gluons having momenta $k_\perp \gg \ell_\perp$ contribute not at all to the charge correlator.

In Sec.6 we present a simple picture which leads to the results quoted for $\frac{dxG}{d^2bd^2\ell}$ and for $\frac{d}{dY}\rho(\ell_\perp, Y)$. This picture is most easily explained by referring to Figs. 5 and 6 where the saturation region is shown. In Fig.5 the saturation region is illustrated for fixed coupling in the y and $\ell n k_\perp^2/\Lambda^2$ plane. Note that y increases in the downward direction in the figure. The diagonal line is the separation line between the dilute and dense regimes. In Fig.6 the saturation region is shown as a function of x_- and y in the Kovchegov gauge[6]. (This picture is that first given by Iancu, Leonidov and McLerran[7] where a gauge was used which puts all the gluons in saturation at positive values of x_- , rather than the choice here of negative values of x_- [6, 8].) In terms of these figures, gluons contributing to $\frac{d}{dY}\rho(\ell_\perp, Y)$ are located in the shaded region C and they come by direct bremsstrahlung emission from the shaded region A. In the region A, ℓ_\perp is the saturation momentum of that rapidity and so the sources at A do not have strong shielding on the scale ℓ_\perp and thus the gluons they emit into region C, having a comparable transverse momentum ℓ_\perp , are also not far from random in color. This naturally gives $\frac{d}{dY}\rho(\ell_\perp, Y) \propto \ell_\perp^2$ with the $1/\alpha$ density of sources being cancelled by the α for a gluon emission leaving $\frac{d}{dY}\rho$ independent of α . Gluons can come into the region C from regions other than A but they do not contribute to $\frac{d}{dY}\rho$ because they are strongly shielded, as explained in Sec.6.

Now turn to $\frac{dxG}{d^2bd^2\ell}$, evaluated at Y . Such gluons come generically from

anywhere along the saturation line in Fig.5, the region B being typical. In Sec.6 we show how emissions from the saturation line, between $Y(\ell_\perp)$ and Y , naturally lead to $\frac{dxG}{d^2\ell_\perp d^2b} \sim \frac{1}{\alpha} \cdot \ln[Q_s^2(Y)/\ell_\perp^2]$ [2, 8, 9, 8].

Finally, in Sec. 6 we show how the x_- – distribution of saturated gluons, as shown in Fig.6, naturally leads to a Glauber-like picture of the scattering of a color dipole on a saturated wavefunction. In passing the saturated hadron the dipole encounters, in a sequential manner, gluons located at different rapidities and scatters independently off them thus naturally leading to the exponential result required by the Balitsky-Kovchegov equation[11, 12, 13].

2 The McLerran-Venugopalan model[1-3]

2.1 The valence quark approximation

In the leading approximation the wavefunction of a high momentum large nucleus consists of the valence quarks of the various nucleons of the nucleus Lorentz-contracted to a thin disc. So long as transverse distances less than a fermi are considered the quarks may be viewed as uncorrelated in color. At an impact parameter b from the center of the nucleus the number of valence quarks per unit area is

$$N(b) = N_0 N_c 2\sqrt{R^2 - b^2} \quad (1)$$

where N_0 is the nuclear density, the number of nucleons per unit volume in the rest system of the nucleus, N_c is the number of colors, and R is the radius of the nucleus. Throughout this paper we take a simplistic view of a nucleus as having a uniform density, N_0 , of nucleons within a sphere of radius R .

Suppose we take the nucleus to be moving along the positive z -axis. Now scatter a left-moving quark-antiquark dipole, moving along the negative z -axis, on the nucleus. The probability that the dipole pass through the nucleus without interacting is equal to

$$S^2(b, x_\perp) = e^{-N(b)\sigma_q(x_\perp)} \quad (2)$$

$$\sigma_q = \left. \begin{array}{c} \text{---} \\ \text{---} \\ \text{---} \end{array} \right\} \mathbf{x}_\perp + \left. \begin{array}{c} \text{---} \\ \text{---} \\ \text{---} \end{array} \right\} \mathbf{x}_\perp$$

Figure 1:

where x_\perp is the transverse separation of the quark-antiquark pair of the dipole and S is the S-matrix for elastic scattering of the dipole with the nucleus. σ_q is the cross-section for scattering of the dipole on a single quark which we take to be [14]

$$\sigma_q(x_\perp) = \frac{\pi^2 \alpha}{N_c} x_\perp^2 x G_q(x, 1/x_\perp^2) \quad (3)$$

where the gluon distribution in a quark is given as

$$x G_q(x, 1/x_\perp^2) = \frac{\alpha C_F}{\pi} \ell n \left(\frac{r_0^2}{x_\perp^2} \right) \quad (4)$$

in the two-gluon exchange approximation illustrated in Fig.1. In (4) r_0 is the radius of a nucleon and we always suppose that $x_\perp^2/r_0^2 \ll 1$. The S-matrix can be written as

$$S = e^{-x_\perp^2 \bar{Q}_s^2/4} \quad (5)$$

where the saturation momentum measured by quarks is given as

$$\bar{Q}_s^2 = C_F/N_c Q_s^2 \quad (6)$$

and where [9] the gluon saturation momentum is

$$Q_s^2 = \frac{4\pi^2\alpha}{N_c^2 - 1} N(b)xG(x, Q_s^2) \quad (7)$$

with the gluon distribution of a nucleon xG given by

$$xG((x, Q_s^2) = N_c xG_q(x, Q_s^2). \quad (8)$$

Finally, the color charge correlator in the nucleus takes the form[15]

$$\langle \rho^i(b + x_\perp)\rho^j(b) \rangle_{MV} = \frac{\delta_{ij}}{N_c^2 - 1} \delta^2(x_\perp) g^2 C_F N(b) \quad (9)$$

where we use a normalization such that

$$\langle \rho^i(b + x_\perp)\rho^j(b) \rangle_{quark} = \delta_{ij} \delta^2(x_\perp) \frac{g^2}{2N_c} \quad (10)$$

for the color correlator of a single high momentum quark.

2.2 Valence quarks along with Weizsäcker-Williams gluons

The valence quarks of a fast nucleus can emit (virtual) gluons which then form the gluon distribution of the nucleus in the semiclassical, Weizsäcker-Williams, approximation. The well-known result for the distribution of gluons is[2, 8]

$$\frac{dxG_A}{d^2\ell_\perp d^2b} = \int \frac{d^2x_\perp}{4\pi^4} \frac{N_c^2 - 1}{\alpha N_c x_\perp^2} (1 - e^{x_\perp^2 Q_s^2/4}) e^{i \ln_\perp \cdot x_\perp} \quad (11)$$

or

$$\frac{dxG_A}{d^2\ell_\perp d^2b} \approx \frac{N_c^2 - 1}{4\pi^3 \alpha N_c} \ell(Q_s^2 / \ln_\perp^2). \quad (12)$$

$\frac{(2\pi)^3}{2(N_c^2-1)} \frac{dxG_A}{d^2\ell_\perp d^2b}$ is the occupation number of gluons, per unit of rapidity. We believe (12), except for overall normalization, is a general result for the phase space density of gluons deep in the saturation regime, $\ell_\perp^2/Q_s^2 \ll 1$, of a high energy wavefunction[9, 10].

Now consider the scattering of a dipole on the nucleus, including the semi-classical gluons in the wavefunction of the nucleus. We wish to determine how (5) and (9) change in the presence of the Weizsäcker-Williams gluons in the nucleus. The calculation is most easily done by Lorentz transforming the dipole-nucleus system so that the dipole carries a greater momentum and the nucleus a lesser momentum. In this way we may view the Weizsäcker-Williams gluons involved in the interaction as being part of the wavefunction of the dipole. The scattering which modifies (5) now can be taken to be that of a left-moving quark-antiquark-gluon system on a McLerran-Venugopalan nucleus having only valence quarks in its wavefunction. In the large N_c limit this contribution, δS , is given by

$$\delta S(b, x_\perp) = \Delta Y \frac{\alpha N_c}{2\pi^2} \cdot \int \frac{d^2 z_\perp x_\perp^2}{(x_{1\perp} - z_\perp)^2 (z_\perp - x_{2\perp})^2} S(b, x_{1\perp} - z_\perp) S(b, z_\perp - x_{2\perp}) \quad (13)$$

and is illustrated in Fig.2. Deep in the saturation regime, $\bar{Q}_s^2 x_\perp^2 \gg 1$, the dominant contribution to (13) comes when $z_\perp = \frac{x_{1\perp} + x_{2\perp}}{2}$. One finds

$$\delta S(b, x_\perp) = \frac{16\alpha N_c}{\pi} \frac{\Delta Y}{\bar{Q}_s^2 x_\perp^2} e^{-x_\perp^2 \bar{Q}_s^2/8} \quad (14)$$

where ΔY is the range of rapidity of the gluons we are considering. Eq.14 shows that the transmission amplitude actually grows and becomes greater for a quark-antiquark-gluon to pass through the nucleus without interaction than for a quark-antiquark to pass through without interaction. In the frame in which we have done the calculation the extra gluon tends to shield the charges in the dipole.

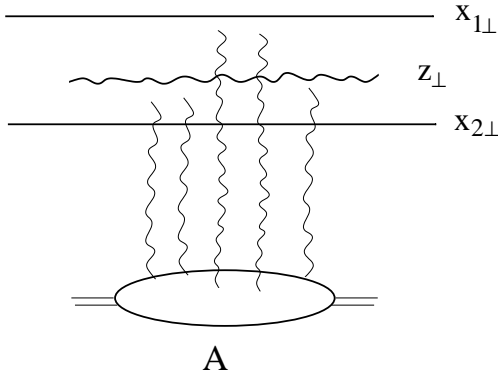


Figure 2:

In a frame where the Weiszäcker-Williams gluons are in the nuclear wavefunction, and (14) is given by the gluon dependent part of the scattering of a quark-antiquark dipole on the nuclear wavefunction, the shielding is expressed by

$$\langle \rho^i(x_{\perp} + b)\rho^j(b) \rangle_{WW} = \frac{1}{2} \langle \rho^i(x_{\perp} + b)\rho^j(b) \rangle_{MV} . \quad (15)$$

This shielding continues to grow as more and more gluons are created. The McLerran-Venugopalan valence quark model seems to be a good starting point for calculating the density of gluons in the saturation region, as given by (11) and (12), but it is not a good starting point for evaluating the distribution of color charge in a large nucleus. In the McLerran-Venugopalan model charges are randomly distributed while in the actual wavefunction there is an arrangement of the quarks and gluons so as to give strong color shielding. Eq.(15), or (14), is the first indication of that shielding.

3 The BFKL wavefunction

The BFKL[4, 5] wavefunction in a dilute (non-saturation) regime already exhibits the charge shielding which we shall find in the saturation regime at extremely high energies. The gluon distribution in the BFKL wavefunction of a high-energy hadron is related to the charge correlator of gluons at all higher rapidities by

$$\frac{dxG}{d^2\ell_\perp} = \frac{1}{4\pi^3\ell_\perp^2} \rho(\ell_\perp, Y). \quad (16)$$

Our notation is such that

$$\rho(\ell_\perp, Y) = \int d^2x_\perp e^{-i\ell_\perp \cdot x_\perp} \sum_i \langle \rho^i(b+x_\perp) \rho^i(b) \rangle d^2b \quad (17)$$

and where the Y variable now indicates a dependence on rapidity in contrast to the McLerran-Venugopalan model. Using

$$\frac{dxG}{d^2\ell_\perp} = c \frac{e^{(\alpha_P-1)Y}}{\sqrt{\alpha Y}} \frac{1}{\ell_\perp} \quad (18)$$

for fixed coupling BFKL evolution one finds

$$\rho(\ell_\perp, Y) = 4\pi^3 c \ell_\perp \frac{e^{(\alpha_P-1)Y}}{\sqrt{\alpha Y}}. \quad (19)$$

The corresponding result using (9) is

$$\rho_{MV}(\ell_\perp) = g^2 C_F \cdot N_q \quad (20)$$

with N_q the total number of quarks in the nucleus. Aside from the Y -dependence in (19), which one expects will disappear in the saturation regime, the big difference between (19) and (20) is that ρ_{MV} has no dependence on ℓ_\perp while the BFKL correlator grows linearly with ℓ_\perp . The lack of an ℓ_\perp -dependence in ρ_{MV} is natural and expresses the fact that the quarks are completely uncorrelated in color in our short distance approximation. The growth of the BFKL correlator with ℓ_\perp , as given by (19), indicates strong color shielding. The linear growth in ℓ_\perp in (19) means that source gluons having $k_\perp \ll \ell_\perp$ contribute little to $\rho(\ell_\perp, Y)$ since there are too few such gluons while source gluons having $k_\perp \gg \ell_\perp$ contribute little to $\rho(\ell_\perp, Y)$ so

that such high momentum gluons are perfectly shielded. Consider an “area” in momentum space $\Delta\ell_\perp^2 = \lambda\pi\ell_\perp^2$, then

$$\frac{d/dY\rho(\ell_\perp, Y)}{\Delta\ell_\perp^2 dxG/d^2\ell_\perp} = \frac{(2\pi)^2}{\lambda} (\alpha_P - 1) \quad (21)$$

being independent of Y and ℓ_\perp indicates that source gluons having $k_\perp \approx \ell_\perp$ contribute essentially independently and incoherently to the charge correlator.

Thus the picture of the distribution of color charges in a BFKL wavefunction is quite simple. Gluons having momentum ℓ_\perp appear as completely shielded by other gluons having a similar momentum when viewed on a scale $\Delta x_\perp > 1/\ell_\perp$ while they appear as completely random charges when viewed on a scale $\Delta x_\perp < 1/\ell_\perp$ with the transition between the two pictures occurring at $\Delta x_\perp \approx 1/\ell_\perp$. We shall see that this picture is preserved in the saturation region where BFKL evolution no longer applies.

4 The light-cone wavefunction in the saturation regime

To deal with the saturation regime we use the Kovchegov equation[12]. (The Balitsky equation[11] would give the same results.) We take the equation in the form, with $x_\perp = x_{1\perp} - x_{2\perp}$,

$$\frac{dS(x_\perp, b, Y)}{dY} = \frac{\alpha C_F}{\pi^2} \int \frac{d^2 z_\perp x_\perp^2}{(x_{1\perp} - z_\perp)^2 (z_\perp - x_{2\perp})^2} \cdot [S(x_{1\perp} - z_\perp, b, Y)S(z_\perp - x_{2\perp}, b, Y) - S(x_\perp, b, Y)], \quad (22)$$

as illustrated in Fig.3. We suppose the vertices in the upper parts of the graphs are taken in the large N_c limit, though of course we cannot assume a large N_c limit for all the graphs as unitarity effects would be lost. We write C_F rather than $N_c/2$ in the prefactor in (22) because that is exact for the virtual correction which will dominate our result. The factorized form of the two S 's on the righthand side of (22), which was originally motivated by

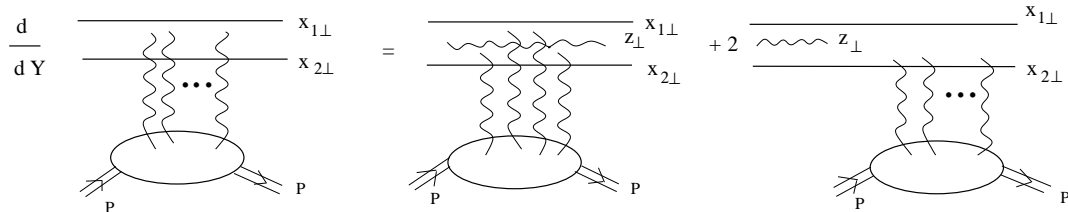


Figure 3:

Kovchegov by choosing scattering on a large nucleus, cannot be expected to be exact, but this will not be important for the argument which follows.

If $Q_s^2(Y)x_{\perp}^2 \gg 1$ the quadratic term in (22) is small when $(x_{1\perp} - z_{\perp})^2 Q_s^2$ and $(x_{2\perp} - z_{\perp})^2 Q_s^2$ are both greater than 1. Thus the dominant contribution to the righthand side of (22) comes from the second term in the regions

$$1/Q_s^2 \ll (x_{1\perp} - z_{\perp})^2 \ll x_{\perp}^2 \quad (23)$$

and

$$1/Q_s^2 \ll (x_{2\perp} - z_{\perp})^2 \ll x_{\perp}^2 \quad (24)$$

giving

$$\frac{dS(x_{\perp}, b, Y)}{dY} = -\frac{2\alpha C_F}{\pi} \ln[Q_s^2 x_{\perp}^2] S(x_{\perp}, b, Y). \quad (25)$$

Using

$$\ln[Q_s^2(Y)/Q_s^2(Y_0)] \approx c \frac{\alpha N_c}{\pi} (Y - Y_0) \quad (26)$$

with [9, 16, 17]

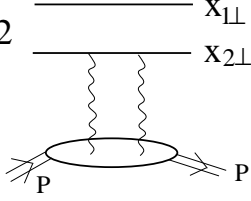
$$\frac{1}{2c} \ln^2 [Q_s^2 x_\perp^2] = 2$$


Figure 4:

$$c = \frac{2\chi(\lambda_0)}{1 - \lambda_0} \quad (27)$$

where $\chi(\lambda)$ is the usual eigenvalue function appearing in BFKL evolution, and λ_0 is determined by $\frac{\chi'(\lambda_0)}{\chi(\lambda_0)} = -\frac{1}{1-\lambda_0}$. Thus[13]

$$S(x_\perp, b, Y) = \exp \left\{ \frac{-C_F}{cN_c} \ln^2 [Q_s^2(b, Y)x_\perp^2] \right\} S(x_\perp, b, Y(x_\perp)), \quad (28)$$

where $Q_s^2(Y(x_\perp)) = 1/x_\perp^2$.

Moving again to a frame where the gluon at z_\perp in (22) and in Fig.3 is in the wavefunction of the hadron on which the dipole scatters, it is natural to identify the exponent in (28) as the scattering, due to two gluon exchange, of the dipole on the saturated hadron. This gives

$$\frac{C_F}{cN_c} \ln^2 [Q_s^2(Y, b)x_\perp^2] = 2 \cdot \frac{g^2}{2N_c} \int_{1/x_\perp^2}^{Q_s^2} \frac{d^2 \ell_\perp}{[\ell_\perp^2]^2} \frac{\rho(\ell_\perp, b, Y)}{4\pi^2} \quad (29)$$

as illustrated in Fig.4 while Eq.29 gives

$$\rho(\ell_\perp, b, Y) = \frac{2C_F}{c\alpha} \ell_\perp^2 \ln [Q_s^2/\ell_\perp^2], \quad (30)$$

where c is given in (27). Now (16) is no longer exactly valid, however, as we shall see in Sec.6, it does continue to have approximate validity. Using (16) with an undetermined constant k gives

$$\frac{dxG}{d^2bd^2\ell_\perp} = k \frac{N_c^2 - 1}{4\pi^3\alpha N_c} \frac{1 - \lambda_0}{2\chi(\lambda_0)} \ell n Q_s^2 / \ell_\perp^2. \quad (31)$$

This result is exactly the same as that found in Ref.9 and except for the way the constants are written that of Ref.10 and of the original McLerran-Venugopalan model, (12). We believe it to be a very general result.

5 Saturation with a running coupling

In this section we shall generalize the results of Sec.4 to the case of QCD with a running coupling. We begin with the generalization of (25) to the running coupling case which now reads

$$\frac{dS(x_\perp, b, Y)}{dY} = -\frac{2C_F}{\pi b} \ell n \left[\frac{\ell n Q_s^2 / \Lambda^2}{-\ell n x_\perp^2 \Lambda^2} \right] S(x_\perp, b, Y). \quad (32)$$

The analogue of (26) is[16, 17]

$$\ell n \left[\frac{Q_s^2(Y, b)}{\Lambda^2} \right] = \sqrt{\frac{2N_c}{\pi b} c Y} + O(Y^{1/6}) \quad (33)$$

where c is exactly as given by (27). Combining (33) with (32) yields

$$S(x_\perp, b, Y) = \exp \left\{ \frac{-C_F}{2cN_c} \left[2 \ln^2 Q_s^2 / \Lambda^2 \ln \left(\frac{\ln Q_s^2 / \Lambda^2}{-\ln x_\perp^2 \Lambda^2} \right) - \ln Q_s^2 x_\perp^2 \ln \frac{Q_s^2}{x_\perp^2 \Lambda^4} \right] \right\} \cdot S(x_\perp, b, Y(x_\perp)) \quad (34)$$

which now replaces (28).

Using the exponent in (34) to identify ρ , exactly as was done in (29), gives

$$\rho(\ell_{\perp}, b, Y) = \frac{2C_F}{c} \langle \frac{1}{\alpha} \rangle \ell_{\perp}^2 \ln[Q_s^2/\ell_{\perp}^2] \quad (35)$$

with

$$\langle \frac{1}{\alpha} \rangle = \frac{1}{2} \left[\frac{1}{\alpha(Q_s^2)} + \frac{1}{\alpha(\ell_{\perp}^2)} \right]. \quad (36)$$

Finally using (16), but again with an undetermined constant, k ,

$$\frac{dxG}{d^2bd^2\ell_{\perp}} = k \frac{N_c^2 - 1}{4\pi^3 N_c} \langle \frac{1}{\alpha} \rangle \frac{1 - \lambda_0}{2\chi(\lambda_0)} \ln Q_s^2/\ell_{\perp}^2 \quad (37)$$

as in (31) except for the replacement $\frac{1}{\alpha} \rightarrow \langle \frac{1}{\alpha} \rangle$.

Thus running coupling effects do not essentially change (30) and (31) which now take the forms (34) and (36), respectively.

6 A simple physical picture

In this section we present a simple physical picture of $\rho(\ell_{\perp}, b, Y)$ and of $\frac{dxG}{d^2bd^2\ell_{\perp}}$ in terms of which gluons in the saturated wavefunction can be viewed as determining ρ and $\frac{dxG}{d^2bd^2\ell_{\perp}}$. The picture is complementary to the picture given in Ref.9 where $\frac{dxG}{d^2\ell_{\perp}d^2b}$ was given a simple interpretation in terms of scattering of a gluon dipole on a hadron. In Fig.5 we exhibit the region of gluons in saturation using the fixed coupling boundary given in (26). We shall carry out the discussion in a fixed coupling context, however, the picture is identical for the running coupling case. In Fig.5 the higher momentum gluons are at the top of the figure, with small values of y , while softer gluons are at the bottom of the figure with large values of y . In Fig.6 we plot the x_{\perp} extent of the gluons in the wavefunction using the Kovchegov gauge[6] where final state rescatterings of produced gluons are absent. The x_{\perp} boundary of the gluons in Fig.6 is [7] $x_{\perp} P_{+} \approx -e^y$ where P_{+} is the momentum of the hadron.

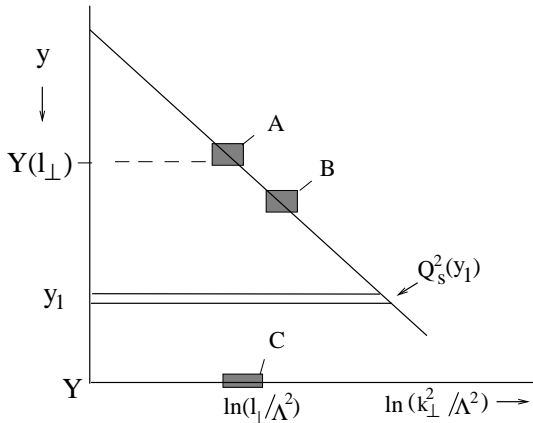


Figure 5:

We begin our discussion by considering $d\rho/dY$ which, from (30) and (26), is

$$\frac{d\rho(\ell_{\perp}, b, Y)}{dY} = \frac{N_c^2 - 1}{\pi} \ell_{\perp}^2. \quad (38)$$

The gluons contributing to (38) come directly from parent gluons located in the region A of Fig.5. Region A is at the edge of the saturation boundary and is of size $\Delta\ell_{\perp} \sim \ell_{\perp}$, $\Delta y \sim 1/(\alpha N_c)$. Thus there are on the order of $\frac{(N_c^2-1)\ell_{\perp}^2}{(\alpha N_c)^2}$ gluons per unit area in A. These gluons emit on the order of $\frac{(N_c^2-1)\ell_{\perp}^2}{(\alpha N_c)^2} \cdot \alpha N_c$ gluons per unit area and per unit rapidity directly into the region $y \approx Y$, $k_{\perp} \approx \ell_{\perp}$. On a scale ℓ_{\perp} these gluons are essentially uncorrelated in color leading to

$$\frac{d}{dY}\rho(\ell_{\perp}, b, Y) \sim (N_c^2 - 1)\ell_{\perp}^2 \quad (39)$$

agreeing with (38). Two natural questions arise. (i) Why not include emissions from other areas, such as region B of Fig.5? Why are there no secondary emissions starting from A? That is a source lying in A could emit a gluon at transverse momentum on the order of ℓ_{\perp} and at rapidity y_1 , lying between $Y(\ell_{\perp})$ and Y , and this gluon could then emit a secondary gluon having ℓ_{\perp} and Y . The answer to (i) is that gluons coming from region B are highly

shielded on a scale ℓ_\perp and contribute little to charge correlations, although, as we shall see shortly they do contribute to the total number of gluons at ℓ_\perp and Y . The answer to (ii) is that gluons emitted from y_1 will typically have transverse momentum on the order of $Q_s(Y_1)$. The probability that a gluon be emitted from ℓ_\perp, y_1 to ℓ_+, Y is proportional to $\ell_\perp^2/Q_s^2(y_1) \ll 1$. Thus the gluons that contribute to $\frac{d\rho(\ell_\perp, b, Y)}{dY}$ are themselves gluons having transverse momentum on the order of ℓ_\perp and which come by direct emission from the region near $\ell_\perp, Y(\ell_\perp)$ where $Q_s[Y(\ell_\perp)] = \ell_\perp$.

Next we turn to $\frac{dxG}{d^2\ell_\perp d^2b}$ evaluated at Y . Now gluons coming from sources having rapidities between $Y(\ell_\perp)$ and Y are important. Focus on sources at rapidity y_1 . We can expect a contribution of size

$$\frac{dxG}{d^2b} \sim \frac{Q_s^2(y_1)}{\alpha} \cdot \alpha \cdot \frac{d^2\ell_\perp}{Q_s^2(y_1)} \cdot dy_1 \quad (40)$$

coming from source in a range dy_1 . Of the four factors on the right-hand side of (40) the first, Q_s^2/α , is the number of gluons per unit area and per unit rapidity at y_1 . The second factor, α , is the strength of emission of gluons from y_1 . $d^2\ell_\perp/Q_s^2$ is the probability that the emitted gluon end up in the momentum range $d^2\ell_\perp$. (Recall that in the Kovchegov light-cone gauge a gluon emitted from y_1 is gauge rotated, locally, by all gluons having larger values of x_- [8], that is essentially by all gluons having rapidities greater than y_1 as is clear from Fig.6. These gauge rotations make the typical transverse momentum of gluons emitted from sources at y_1 on the order of $Q_s(y_1)$.) dy_1 is the range of sources in rapidity. Integrating dy_1 between $Y(\ell_\perp)$ and Y gives [9, 10]

$$\frac{dxG}{d^2\ell_\perp d^2b} \sim [Y - Y(\ell_\perp)] = \frac{\pi}{\alpha N_c} \frac{1 - \lambda_0}{2\chi(\lambda_0)} \ln \frac{Q_s^2(y)}{\ell_\perp^2} \quad (41)$$

which contains the essential factors in (31) and (35). It is important to note that the gluons contributing to (39) are highly correlated in color. If they were randomly distributed in color they would lead to a contribution

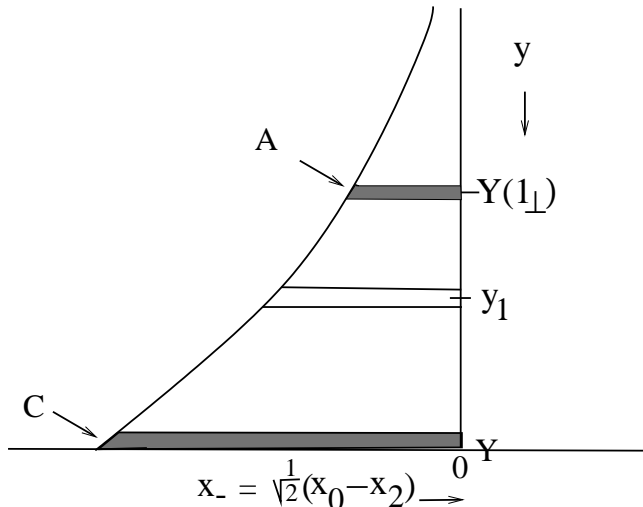


Figure 6:

to $\frac{d\rho(\ell_\perp, b, Y)}{dY}$ of size $\alpha[Y - Y(\ell_\perp)] \sim \ln[Q_s^2(Y)/\ell_\perp^2]$ which is too large. Because the sources from which most of the gluons in (41) come from are strongly shielded on scale ℓ_\perp the gluons in (41) should themselves contribute little to $\rho(\ell_\perp, b, Y)$. Finally, gluon sources at y_1 having momentum $k_\perp \ll Q_s(y_1)$ are too few in number to contribute to (40) while gluon sources having $k_\perp \gg Q_s(y_1)$ are too strongly shielded to be important.

It is interesting to carry out one last calculation which helps explain why (28) and (34) have all Y -dependence occurring in the exponent. To that end we turn to an interpretation of (25). In the Kovchegov picture the fact that $\frac{dS}{dY}$ is proportional to S comes about because the virtual correction shown in Fig.3 occurs long before the actual scattering, the term shown in the figure, or long after the scattering. The exponential result then comes about because the virtual gluon corrections are ordered in time, according to the longitudinal momentum of the gluons, thus naturally leading to an exponential result. How does this occur in a picture where the Y -dependence is put into the target rather than in the dipole? When the rapidity of the target is increased by dY , there is an increase in the charge correlator by $d\rho(\ell_\perp, b, Y)$ and this increased charge is located at “large” negative values of x_- as shown in the shaded part of Fig.7 where the top part of that figure shows the distribution of charge as a function of Y , much as in Fig.6. Also

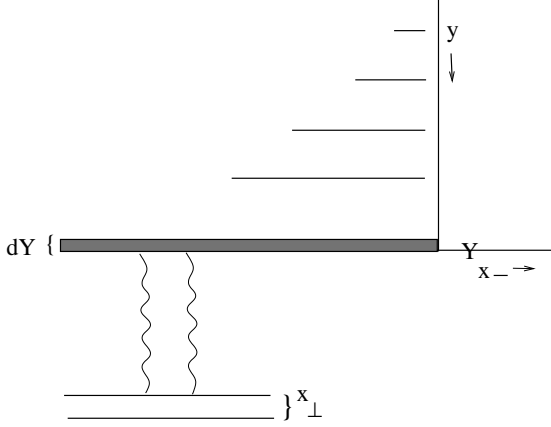


Figure 7:

shown is a scattering off that additional charge by the dipole which reaches the charge in $d\rho$ before it reaches the charge located at higher rapidities. There must be at least two gluons exchanged because the charges located at different rapidities are too weakly correlated to give a non-zero result and there will be no more than two gluons going from dY to the dipole since the coupling to the charge in dY is not very large unless dY is quite big. More precisely we can rewrite (25) as

$$\frac{dS}{dY}(x_{\perp}, b, Y) = - \int \frac{d\rho(\ell_{\perp}, b, Y)}{dY} \frac{d^2\ell_{\perp}}{4\pi^2[\ell_{\perp}^2]^2} \cdot 2 \cdot \frac{g^2}{2N_c} S(x_{\perp}, b, Y). \quad (42)$$

The factors on the righthand side of (42) are: $g^2/2N_c$ is the coupling of two gluons to one of the quarks in the dipole; the 2 counts the number of quarks in a dipole while $\frac{1}{4\pi^2} \frac{d^2\ell_{\perp}}{[\ell_{\perp}^2]^2}$ gives the phase space and propagators. $S(x_{\perp}, b, Y)$ then corresponds to the later, in time, scatterings with the rest of the charge in the hadron's wavefunction. The integral in (40) goes from $\ell_{\perp} = 1/x_{\perp}$ to $\ell_{\perp} = Q_s(Y)$. Using (38) then leads to (25).

References

- [1] L. McLerran and R. Venugopalan, Phys. Rev.**D49** (1994) 2233; **D49** (1994) 3352; **D50** (1994) 225.
- [2] J. Jalilian-Marian, A. Kovner, L. McLerran and H. Weigert, Phys. Rev. **D55** (1997) 5414.
- [3] Yu. V. Kovchegov, Phys. Rev. **D54** (1996) 5463.
- [4] E.A. Kuraev, L.N. Lipatov and V.S. Fadin, Sov.Phys. JETP, **45** (1977) 199.
- [5] Ya.Ya. Balitsky and L.N. Lipatov, Sov.J. Nucl.Phys.**28** (1978)822.
- [6] Yu. V. Kovchegov, Phys. Rev. **D55** (1977) 5445.
- [7] E. Iancu, A. Leonidov and L. McLerran, Phys. Lett. **B510** (2001)133; Nucl. Phys. **A692** (2001) 583.
- [8] Yu. V. Kovchegov and A.H. Mueller, Nucl.Phys. **B529** (1998) 451.
- [9] A.H. Mueller, Nucl.Phys. **B558** (1999) 285.
- [10] E. Iancu and L. McLerran, Phys. Lett. **B510** (2001) 145.
- [11] I.I. Balitsky, Nucl. Phys. **B463** (1996) 99; Phys. Rev.Lett. **81** (1998) 2024; Phys. Lett. **B518** (2001) 235.
- [12] Yu. V. Kovchegov, Phys. Rev.**D60** (1999) 034008; **D61** (2000) 07418.
- [13] E.M. Levin and K. Tuchin, Nucl.Phys. **B573** (2000) 83.
- [14] B. Blättel, G. Baym, L.L. Frankfurt and M. Strikman, Phys. Rev.Lett. **70** (1993) 896.
- [15] E. Iancu, A. Leonidov, L. McLerran, hep-ph/0202270.
- [16] A.H. Mueller and D.N. Triantafyllopoulos, hep-ph/0205167.
- [17] E. Iancu, K. Itakura and L. McLerran, hep-ph/0203137.